

Model of Linear Quadratic Regulator (LQR) Control System in Waypoint Flight Mission of Flying Wing UAV

Tri Kuntoro Priyambodo¹, Oktaf Agni Dhewa¹ and Try Susanto²

¹Departmen of Computer Science and Electronics, Universitas Gadjah Mada.

²Departmens of Informatics Engineering, Universitas Teknokrat Indonesia.

mastri@ugm.ac.id

Abstract—The ability of the aircraft to trace the waypoint trajectory is a major requirement for the completion of various missions. However, the magnitude of steady state error and multiple overshoot caused by environmental disturbances can cause instable motion of the aircraft. Such conditions can make the aircraft experience a shift and change its direction from a predetermined path. Therefore, in this study Linear Quadratic Regulator (LQR) control method is applied to minimize steady state error and multiple overshoot. The LQR control method has the ability to maintain the stability of the aircraft and produce minimum errors. Besides, the LQR control method can also be modified by providing input references so that it can be used for tracking trajectories. System testing is done directly on tracing the triangular trajectory pattern to find out directly the functioning of the system. The results derived from the testing of the model design indicated a steady state tendency of 3.55% error, with the largest deviation of 10.55% and 83% accuracy for tracking from the first waypoint to the second waypoint. It was also reported a steady state tendency of 2.88% error, the largest deviation of 7.28% with 93% accuracy for tracing from the second waypoint to the third waypoint.

Index Terms—Optimal Control; Stability; UAV; Waypoint.

I. INTRODUCTION

The development of UAV (Unmanned Aerial Vehicle) or aircraft technology Unmanned is increasingly developing with the increasing use of UAVs in the world [1] [2] [3]. Unmanned aircraft can be used for monitoring, search and rescue missions and even for ambushes in conditions of war [4]. To complete these missions, the UAVs are required to fly independently (autopilot) to trace the flight path in accordance with the row of coordinates of the location of the earth that has been determined, which is often referred to as the waypoint mission [5][6].

Many UAVs have experienced changes in the physical form of manufacturing. One type of unmanned aircraft is the flying wing model. This type of aircraft has a fixed wing in the form of a triangle, which is equipped with two servo and no tail (tail less). Its configuration is very simple as it consists of wings and control surfaces in the form of aileron or elevator only. This model aircraft is capable of gliding in the air and it consumes minimal power. It is also able to explore with a far range, while carrying cargo in it [7].

To carry out the waypoint missions, UAVs need a navigation system with data information obtained from GPS [8]. GPS will read the longitude and latitude of the earth, which is used as a reference value to get to the point of destination [9]. In addition, UAVs also require control

methods to regulate the configuration of aircraft motion in maintaining flight orientation stability to prevent stalling [10]. PID (Proportional Integral Derivative) control methods have been used to carry out waypoint tracking missions, but its control is not optimal when handling the aircraft in a correct position with large mean deviation error [11] and [12].

The occurrence of these deviations will be accompanied by continuous and large state error or mean deviation. This condition causes the UAV to experience a shift from the track. A large steady state error with an intensity often cause the system to experience multiple overshoots, which result in not only the flight conditions and shifts, but also a change from its traced trajectory [13].

Research conducted by [14] and [15] focuses on controlling the stability of the UAV by implementing a full state feedback Linear Quadratic Regulator (LQR) control method indicates the ability to make the system overcome errors through rapid response. Further, several other studies that focus on the application of LQR control methods on UAV aircraft found more effective way to get a stable system response [16] and that produce minimum errors [17].

This paper aims to design flight performance stability of UAV, especially flying wing construction using LQR method control system. It is expected that the plane can accommodate waypoint mission with a minimal inconvenience.

II. FLYING WING MODEL

The forces acting on a Flying Wing are visualized in Figure 1.

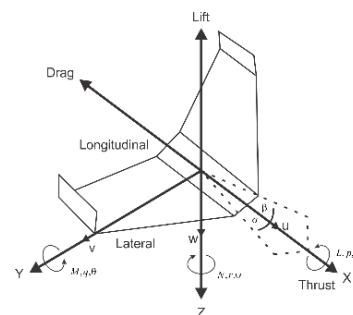


Figure 1: Flying wing UAV model

A. Translation Movement

The determination of aircraft translational motion is conducted by using Newton-Euler law relations, which is based on Newton's second law.

$$\sum F = ma \quad (1)$$

where: $m = \text{mass (kg)}$
 $a = \text{acceleration } (\frac{m}{s^2})$

$$\sum F = F + F_{gravity} \quad (2)$$

$$\sum F = m \frac{d}{dt} v_T = m \frac{d}{dt} v_T + (\omega \times v_T) \quad (3)$$

where : $v_T = \text{translation velocity } (\frac{m}{s})$
 $\omega = \text{angular velocity } (\frac{rad}{s})$

Linear vector velocity and total angular can be calculated in Equations 4 and 5:

$$v_T = iU + jV + kW \quad (4)$$

$$\omega = iP + jQ + kR \quad (5)$$

Thus, the forces that occur on the plane can be written in the following matrix [18]:

$$\omega \times v_T = \begin{bmatrix} i & j & k \\ P & Q & R \\ U & V & W \end{bmatrix} = (QW - VR) + (UR - PW) + (PV - UQ) \quad (6)$$

Based on the earth's gravity force on each plane axis the force of each axis on the plane can be written [19]:

$$X = (U + QW - VR + g \sin \theta) \quad (7)$$

$$Y = (V + UR - PW - g \cos \theta \sin \phi) \quad (8)$$

$$Z = (W + PV - UQ + g \cos \theta \cos \phi) \quad (9)$$

B. Rotation Movement

Rotational motion on a plane is defined through the angular momentum acting on the system. The momentum has the following Equation [18]:

$$H = I\omega \quad (10)$$

where: $H = \text{angular momentum } (\frac{kg.m^2.rad}{s})$
 $I = \text{moment of inertia } (kg.m^2)$

Torque that occurs in the system is:

$$M = I \frac{d}{dt} (\omega + \omega \times \omega) + \omega \times H \quad (11)$$

where: $\omega \times \omega = 0$

So Equation 11 can be Equation (12) and then (13).

$$\frac{d}{dt} \omega = iP + jQ + kR \quad (12)$$

$$\omega \times H = \begin{bmatrix} i & j & k \\ P & Q & R \\ h_x & h_y & h_z \end{bmatrix} \quad (13)$$

The moment of inertia that occurs on all the three axes of

the plane [19] as in Equation (14) with h_x, h_y and h_z as Equations (15)-(17) and (18).

$$H = \begin{bmatrix} I_{xx} & -I_{yy} & -I_{zz} \\ -I_{xy} & I_{yy} & -I_{yz} \\ -I_{xy} & -I_{yz} & I_{zz} \end{bmatrix} \quad (14)$$

$$h_x = -I_{xx}P - I_{xy}Q - I_{xz}R \quad (15)$$

$$h_y = -I_{xy}P + I_{yy}Q - I_{yz}R \quad (16)$$

$$h_z = -I_{xz}P - I_{yz}Q + I_{zz}R \quad (17)$$

$$I \frac{d}{dt} \omega = \begin{bmatrix} I_{xx}\dot{P} & -I_{yy}\dot{Q} & -I_{zz}\dot{R} \\ -I_{xy}\dot{P} & I_{yy}\dot{Q} & -I_{yz}\dot{R} \\ -I_{xy}\dot{P} & -I_{yz}\dot{Q} & I_{zz}\dot{R} \end{bmatrix} \quad (18)$$

The plane has a symmetrical body to the plane XZ then $I_{xy} = I_{yz} = 0$. Therefore, the moment of roll, pitch and yaw can be applied by the Equations:

$$M_x = I_{xx}\dot{P} - (\dot{R} + PQ) + (I_{zz} - I_{yy}) \quad (19)$$

$$M_y = I_{yy}\dot{Q} - (P\dot{R} + R\dot{P}) + (I_{xx} - I_{zz}) \quad (20)$$

$$M_z = I_{zz}\dot{R} - I_{xz}\dot{P} + (I_{xx} - I_{yy} + RQI_{xz}) \quad (21)$$

where: $M_x = L$ (roll)
 M_y is M (pitch)
 M_z is N (yaw)

III. CONTROL SYSTEM DESIGN

The Flying Wing aircraft control system design model is derived from Equations (7)-(9), which are the torque equations in the vehicle. Adjustment of the variables of the flying vehicle into a variable for the aircraft model in this study can be seen in Table 1.

Table 1
Variable Adjustment to Decline Model

Previous Variable	Variable Adjustment	Description
L	τ_1	roll torque
M	τ_2	pitch torque
P	ω_ϕ	roll angular velocity
Q	ω_θ	pitch angular velocity
U	V_x	translation velocity x
V	V_y	translation velocity y
W	V_z	vertical velocity

Based on Table 1, the equation of motion of the x and y axis rotation in Equations (19) and (20) can be adjusted only to the extent of adjusting the variables without changing the equation. So, the equations of rotational motion of the x and y axis can be written in the Equation [20]:

$$I_{xx}\dot{P} + (I_{xz} - I_{yy})\omega_\theta r = \tau_1 \quad (22)$$

$$I_{yy}\dot{Q} + (I_{xx} - I_{zz})\omega_\phi r = \tau_2 \quad (23)$$

where: $I_{xx} = \text{Inertia of the x-axis plane}$

I_{yy} = Inertia of the y-axis plane
 \ddot{p} = Acceleration of roll angle
 \ddot{q} = Acceleration of pitch angle
 τ_1 = Pitch rate
 τ_2 = Roll rate
 r = Yaw rate

Rotational motion on the x and y axes based on Equations (22) and (23) can be modeled as follows:

$$I_{xx}\ddot{p} + (I_{xz} - I_{yy})\omega_\theta r = \tau_1 \quad (24)$$

$$I_{yy}\ddot{q} + (I_{xx} - I_{zz})\omega_\phi r = \tau_2 \quad (25)$$

The system parameters used in this waypoint mission involve 10 controlled states:

- x position and x-axis translation velocity (v_x)
- y position and y-axis translation velocity (v_y)
- z position and z-axis translation velocity (v_z)
- Roll angle (ϕ) and roll angular velocity (ω_x)
- Pitch angle (θ) and pitch angular velocity (ω_y)

So, the shape of the flying wing state space is described in the following equations:

$$\begin{bmatrix} \dot{U} \\ \dot{V} \\ \dot{W} \\ \dot{X}_E \\ \dot{Y}_E \\ \dot{Z}_E \\ \dot{\phi} \\ \dot{\theta} \\ \dot{P} \\ \dot{Q} \end{bmatrix} = \begin{bmatrix} 0 & 1 & 0 & 0 & 0 & 0 & 0 & 0 & 0 & 0 \\ 0 & 0 & 0 & 0 & 0 & 0 & 0 & 0 & 0 & -W \\ 0 & 0 & 1 & 0 & 0 & 0 & 0 & 0 & 0 & 0 \\ 0 & 0 & 0 & 0 & 1 & 0 & 0 & 0 & 0 & W \\ 0 & 0 & 0 & 0 & 0 & 0 & 0 & 0 & 0 & 0 \\ 0 & 0 & 0 & 0 & 0 & 0 & 0 & 0 & 0 & -V \\ 0 & 0 & 0 & 0 & 0 & 0 & 1 & 0 & 0 & 0 \\ 0 & 0 & 0 & 0 & 0 & 0 & 0 & 0 & 0 & 0 \\ 0 & 0 & 0 & 0 & 0 & 0 & 0 & 0 & 0 & \frac{(I_{xz} - I_{yy})}{I_{xx}} \\ 0 & 0 & 0 & 0 & 0 & 0 & 0 & 0 & 0 & 0 \\ 0 & 0 & 0 & 0 & 0 & 0 & 0 & 0 & 0 & \frac{(I_{xx} - I_{zz})}{I_{yy}} \\ 0 & 0 & 0 & 0 & 0 & 0 & 0 & 0 & 0 & 0 \end{bmatrix} \begin{bmatrix} X_E \\ U \\ V \\ Y_E \\ Z_E \\ W \\ \phi \\ \theta \\ P \\ Q \end{bmatrix} + \begin{bmatrix} 0 & 0 & 0 & 0 & 0 & 0 & 0 & 0 & 0 & 0 \\ \frac{1}{m} & 0 & 0 & 0 & 0 & 0 & 0 & 0 & 0 & 0 \\ 0 & 0 & 0 & 0 & 0 & 0 & 0 & 0 & 0 & 0 \\ 0 & \frac{1}{m} & 0 & 0 & 0 & 0 & 0 & 0 & 0 & 0 \\ 0 & 0 & 0 & 0 & 0 & 0 & 0 & 0 & 0 & 0 \\ 0 & 0 & 0 & 0 & 0 & 0 & 0 & 0 & \frac{1}{I_{xx}} & 0 \\ 0 & 0 & 0 & 0 & 0 & 0 & 0 & 0 & 0 & \frac{1}{I_{yy}} \\ 0 & 0 & 0 & 0 & 0 & 0 & 0 & 0 & 0 & 0 \\ 0 & 0 & 0 & 0 & 0 & 0 & 0 & 0 & 0 & 0 \\ 0 & 0 & 0 & 0 & 0 & 0 & 0 & 0 & 0 & 0 \end{bmatrix} \begin{bmatrix} F_x \\ F_y \\ F_z \\ L \\ M \end{bmatrix} \quad (26)$$

$$\dot{x} = Ax + Bu$$

$$\begin{bmatrix} y_1 \\ y_2 \\ y_3 \\ y_4 \\ y_5 \end{bmatrix} = \begin{bmatrix} 1 & 0 & 0 & 0 & 0 & 0 & 0 & 0 & 0 & 0 \\ 0 & 0 & 1 & 0 & 0 & 0 & 0 & 0 & 0 & 0 \\ 0 & 0 & 0 & 0 & 1 & 0 & 0 & 0 & 0 & 0 \\ 0 & 0 & 0 & 0 & 0 & 0 & 1 & 0 & 0 & 0 \\ 0 & 0 & 0 & 0 & 0 & 0 & 0 & 0 & 1 & 0 \end{bmatrix} \begin{bmatrix} X_E \\ U \\ V \\ Y_E \\ Z_E \\ W \\ \phi \\ \theta \\ P \\ Q \end{bmatrix} + \begin{bmatrix} 0 & 0 & 0 & 0 & 0 \\ 0 & 0 & 0 & 0 & 0 \\ 0 & 0 & 0 & 0 & 0 \\ 0 & 0 & 0 & 0 & 0 \\ 0 & 0 & 0 & 0 & 0 \end{bmatrix} \begin{bmatrix} u_1 \\ u_2 \\ u_3 \end{bmatrix} \quad (27)$$

$$y = Cx + Du$$

The LQR control system diagram is as shown below.

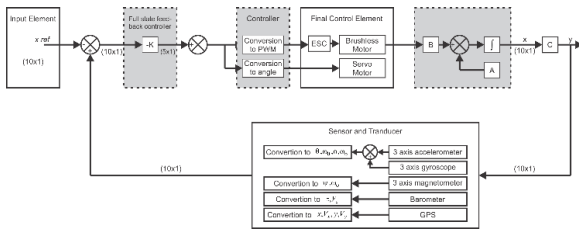


Figure 2: Control system diagram of LQR in flying wing

The inertia of each axis can be calculated using the following equations [18].

$$I_{xx} = \frac{1}{12} m(b^2 + c^2) \quad (28)$$

$$I_{yy} = \frac{1}{12} m(a^2 + b^2) \quad (29)$$

$$I_{zz} = \frac{1}{12} m(a^2 + c^2) \quad (30)$$

The purpose of LQR control is to find the K matrix gain as the feedback gain to optimize the control system. The selection of LQR controls is due to the method that this control minimizes the cost function [21]. LQR control works based on a matrix Q and R to get the best K value in order to maintain flight stability. The weighting process of Q and R matrices is done to get the control response in accordance with the desired control specifications [22].

The value of Q is directly proportional to the value of the auxiliary variable from the Riccati equation (P) for determining the value of K. The value of P is proportional to the reinforcement of the value of K, so the greater the value of Q, the greater the value of K. The weighting of Q and R values starts from value 1, then it will be added or subtracted according to system requirements, but the Q and R constants have opposing functions, if the value of R is large, then the feedback does not really affect the system; therefore the reasoning is only done on the matrix Q, where the matrix R is given a value of 1 so that the value of R does not affect the control [23].

The LQR control system is a control method that is specialized as a regulator. The problem that arises is what if the autonomous system change the state reference. Changing the references with physical quantities from state is not the same as the amount of the input reference. To solve the problem, the state reference (x_{ref}) is given. The provision of the references state will result in Equation 31.

$$\dot{x} = Ax + (-K(x - x_{ref})) \quad (31)$$

IV. ARCHITECTURE SYSTEMS

A. Electronics Design

The sensors used in this system include an accelerometer and a gyroscope that produce data in the form of a roll and pitch angle value. Navigating the aircraft using the compass sensor and maintaining the heading of the aircraft using the barometer provide altitude data with the Kalman Filter method. In addition, this system uses GPS sensors to get the x and y and longitude translational data and earth coordinate data. In this study, the algorithm processing used in the hardware part is the ARM Cortex-M4 microcontroller that is used with computational calculation speeds reaching 72 MHz and it has a flash memory of 256 Kbytes. While the actuator uses a brushless motor with 1400 KV specifications and two servo motors. The relationship between these electronic parts is illustrated in Figure 3.

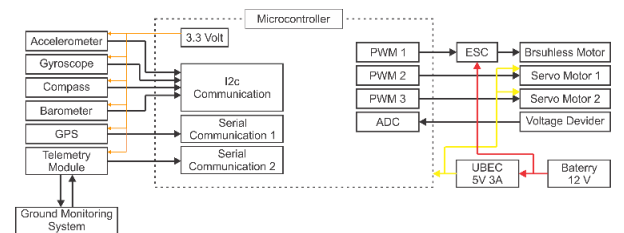


Figure 3: Architecture system

B. Mechanics Design

The aircraft mechanical design made in this study is shown in Figure 4.

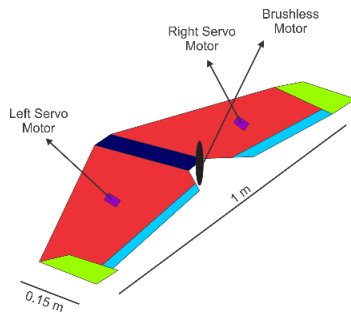


Figure 4: Mechanics design of flying wing

C. Flow Concept Programming

The system will enter the initial conditions for initiating sensor access, remote reading receivers, telemetry and actuators. Then, the system will check whether the aircraft is ready to fly or not. If the system is not ready to fly, any command given will not affect the system of the aircraft. The condition of the aircraft system ready to fly is done by changing the switch mode on the remote. The main program in flight condition will check the subprograms that instruct the aircraft to fly in a stabilized mode, heading mode or waypoint mission mode. When the aircraft system runs all existing conditions, each condition will carry out the calculation of the control of each controlled state.

The main aircraft system program is described in a form of a flowchart as shown in Figure 5.

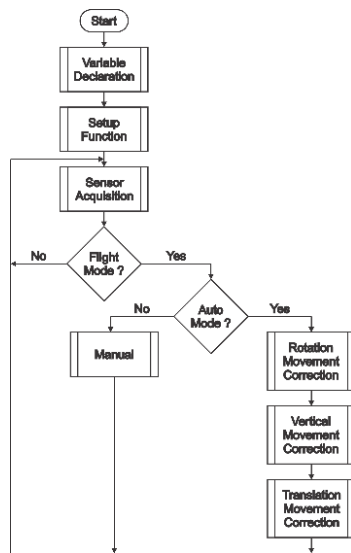


Figure 5: Flow diagram programming
V. FLIGHT SCENARIO

Airplane flight scenarios in tracing waypoint points can be explained based on the following points:

- The flight starts with manual take off by the pilot using a remote control until the plane is headed for a certain height.
- After the aircraft is at a certain height, the pilot will deliver remote plane commands from manual mode to stabilize mode. The mode allows the aircraft to maintain aircraft stability on the axis for roll and axis for pitch.

- Furthermore, the pilot gives commands to the altitude hold mode, this mode allows the aircraft to survive at a certain height automatically.
- Then the pilot will give commands to the aircraft in waypoint mode. In this mode, the plane will fly through the pattern of waypoint points that have been determined.
- When the aircraft has completed the waypoint mission and is at the end point, the flight will then be diverted again by the pilot and controlled manually to make the landing.

Basically, the plane can make translational motion along the x or y axis of the framework body reference. As long as the translation moves along the path on the axis-axis, the plane gets input to roll. The roll will change the direction of flying rides on translational flights. The input is a waypoint coordinate. The waypoint coordinate points put on the plane before the flight mission begins, to be a reference aircraft movement. The aircraft utilizes data from GPS sensors, for comparing the position of the latitude and longitude of the vehicle to the point of destination coordinates, where the feedback of the difference in value will be sent to the control system to set the attitude of the vehicle roll so as to get to the waypoint coordinates of the destination waypoint [24]. In this study, three waypoints and one home point were used to determine the direction towards the waypoint point needed to determine the angle facing the plane to the point destination coordinates [12]. This is called the bearing angle. This angle can be searched by comparing the point coordinates of the destination with the coordinates of the plane, which is shown in Figure 6.

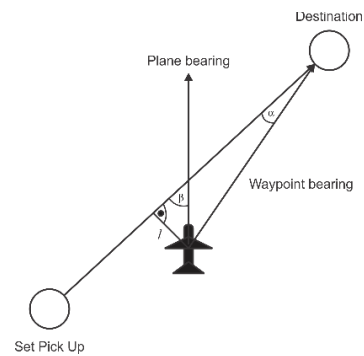


Figure 6: Bearing angle from two different point location [11]

Bearing angles were calculated from the compass angle value of 0 degrees that lead to the north of the earth. The calculation of bearing angles can be described based on the following equation.

$$dLong = Long_{dest} - Long_{act} * \frac{180}{\pi} \tag{32}$$

$$a1 = \sin(dLong) * (Lat_{dest} * \frac{180}{\pi}) \tag{33}$$

$$a2_1 = \sin(Lat_{dest} * \frac{180}{\pi}) * \cos(Lat_{dest} * \frac{180}{\pi}) * \cos(dLong) \tag{34}$$

$$a2 = \cos(Lat_{dest} * \frac{180}{\pi}) * \sin(Lat_{dest} * \frac{180}{\pi}) - a2_1 \tag{35}$$

$$bearing = atan2(a1, a2) \tag{36}$$

where: $dLong$ = Difference between the value of the destination longitude and the actual longitude in the

form of radians

a1 = Value of the earth's axis

a2 = x-axis of the earth's axis.

The calculation of the deviation of the aircraft's position with respect to the waypoint reference is shown in Figure 7.

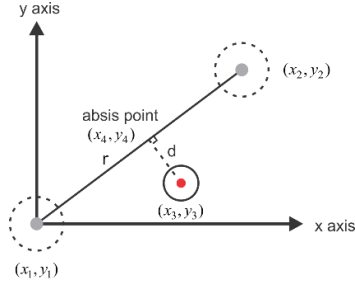


Figure 7: Visualization of aircraft deviation from reference points

The picture above shows that (x_1, y_1) is the first coordinate point of reference for the plane in tracing the path, assuming the x and y axes are the same displacement with 0 meters. The point forms a path along r with respect to (x_2, y_2) , which is the point of destination coordinates. The length of the path r can be obtained through Equations (37)-(41), the point x represents the coordinates of longitude and point y representing latitude coordinates [8].

$$dLon = y_2 - y_1 \quad (37)$$

$$dLat = x_2 - x_1 \quad (38)$$

$$a = \sin^2\left(\frac{dLat}{2}\right) + \cos(y_2) * \cos(y_1) * \sin^2\left(\frac{dLon}{2}\right) \quad (39)$$

$$b = 2 * \text{atan2}(\sqrt{a}, \sqrt{1-a}) \quad (40)$$

$$r = R * b \quad (41)$$

$dLat$ is the value of the difference in the destination latitude with the first latitude, $dLon$ is the difference between the first longitude coordinates and longitude coordinates of the destination, as well as R is the radius of the earth at 6,371.000 meters.

VI. RESULT AND DISCUSSION

A. Roll and Pitch Rotation Response

The stability of the roll and pitch motion of the aircraft is influenced by the state control, namely the angle of orientation and angular velocity of each axis. Each state has a full state feedback gain element obtained from weighting variations, that is the Q element for each state. The Q element of the roll motion state component and the pitch consists of Q_ϕ and Q_p for roll, Q_θ and Q_q to pitch. Q is used to get K_ϕ and K_{ω_ϕ} on the roll, K_θ and K_{ω_θ} on the pitch.

Table 2
Matrix Conversion Q Roll and Pitch to Gain K

Q	K
$\begin{bmatrix} 0 & 0 & 0 & 0 & 0 & 0 & 1.01 & 0 & 0 & 0 \\ 0 & 0 & 0 & 0 & 0 & 0 & 3.92 & 0 & 0 & 0 \\ 0 & 0 & 0 & 0 & 0 & 0 & 0 & 1.69 & 0 & 0 \\ 0 & 0 & 0 & 0 & 0 & 0 & 0 & 0 & 43.49 & 0 \end{bmatrix}$	$\begin{bmatrix} 0 & 0 & 0 & 0 & 0 & 0 & 1 & 2 & 0 & 0 \\ 0 & 0 & 0 & 0 & 0 & 0 & 0 & 0 & 1.3 & 6.6 \end{bmatrix}$

Table 2 shows the best Q value components required

by the system. The best value of K is influenced by the greater weighting variation of Q element, and it will produce a greater K gain value as well. A large K gain value will produce torque on the aircraft system, making the system more responsive [25].

The result of K gain obtained from weighting the value of Q element is proven with the test results as follows.

Table 3
Characteristics Response of Roll Rotation

Response Transient	Result			Minimum Requirement
	Test 1	Test 2	Test 3	
Rise Time (tr)	0.25	0.9	0.18	< 1 s
Settling Time (ts)	0.8	0.7	0.7	< 3 s
Overshoot	1.22	0	1.55	< 4.5 ⁰
Undershoot	0	-1.97	0	> -4.5 ⁰
Steady State Error	-1.37	-0.85	1.01	± 4.5 ⁰

Table 4
Characteristics Response of Pitch Rotation

Response Transient	Result			Minimum Requirement
	Test 1	Test 2	Test 3	
Rise Time (tr)	0.32	0.19	0.29	< 1 s
Settling Time (ts)	1.2	0.7	0.8	< 3 s
Overshoot	1.27	1.3	0.73	< 4.5 ⁰
Undershoot	0	0	0	> -4.5 ⁰
Steady State Error	1.42	0.78	0.75	± 4.5 ⁰

Based on the roll and pitch rotational motion testing, the aircraft already has minimum system stability characteristics. Tests conducted on control both states prove that LQR control is able to maintain stability roll and pitch torque against a given disturbance with eliminated oscillation [27]. The state control process in the rotational motion is the basic thing that must be done to support the system flight as it is able to trace the waypoint points.

B. Vertical Movement Response

The vertical motion characteristics of the aircraft are obtained from giving a K gain to the LQR control over the tuning of the Q parameter position z (Q_z) or the height and speed of the z axis (Q_{v_z}). The best Q tuning results are shown in the following Table 5.

Table 5
Matrix Conversion Q Vertical Movement to Gain K

Q	K
$\begin{bmatrix} 0 & 0 & 0 & 0 & 2.5 & 0 & 0 & 0 & 0 & 0 \\ 0 & 0 & 0 & 0 & 0 & 0.5 & 0 & 0 & 0 & 0 \end{bmatrix}$	$\begin{bmatrix} 0 & 0 & 0 & 0 & 0.2 & 0.22 & 0 & 0 & 0 & 0 \end{bmatrix}$

The designed control has been able overcome the aircraft's attitude in maintaining its altitude. Controlling the vertical position will assist the aircraft in conducting a search. The aircraft will tend to stall when turning in a certain direction if it is not accommodated with vertical motion control.

C. Waypoint Mission Response of Bamboo Flying Wing

Testing aircraft motion to trace the waypoints built by entering the three points on earth's coordinates, and the

latitude and longitude are different. The coordinates of the waypoint points are listed in Table 6.

Table 6
Coordinate Point

WP	Coordinate	
	Latitude	Longitude
1	-7.7517409	110.3478775
2	-7.7500896	100.3484039
3	-7.7503271	110.3497696

Aircraft movement starts from the home point when the waypoint mode is activated. Then, the home point of the plane will go to the first coordinate point (wp1), and then the plane moves to the coordinates (wp2) and ends at (wp3). The path pattern in the stopover sequence at a waypoint station will be traced to the aircrafts that are accommodated using the LQR control system.

The accuracy in tracking the waypoints reflects that LQR control methods are able to accommodate aircraft stability. The accuracy value of the aircraft is obtained based on the position of the aircraft path inside the fault tolerance limit during the flight mission, and the calculation is done with the following equation.

$$Accuracy = \frac{a}{b} * 100 \% \quad (42)$$

where: a = Number of data in boundaries
 b = All of data

The results of testing the LQR control method applied to the waypoint mission provide the characteristics of flight movements, which are detailed in the following table.

Table 7
Characteristics Response of Roll Rotation

No.	Path	Length Path (m)	Devia-tion	Time (s)	SSE	Accuracy
1	wp1 to wp2	165	12.66	13.8	-4.09	87%
	wp2 to wp3	152	7.34	15	-2.62	100%
2	wp1 to wp2	165	15.9	11.1	-4.5	75.4%
	wp2 to wp3	152	0	15	-2.72	100%
3	wp1 to wp2	165	9.33	12.2	-4.2	88.3%
	wp2 to wp3	152	8.74	12.9	-5.03	79%

The best aircraft movement plot is shown in Figure 8.

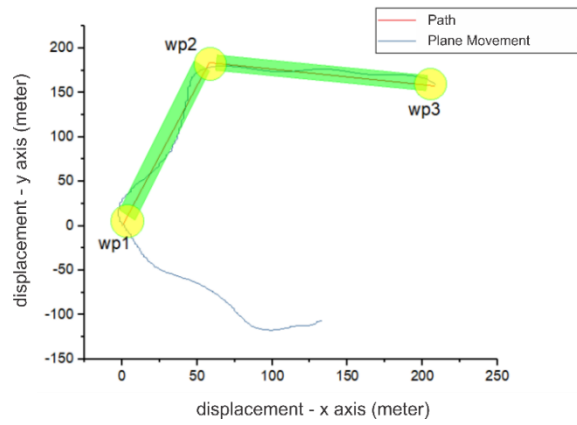


Figure 8: The characteristics movement of aircraft when doing a waypoint flight mission

After several attempts, the best results were obtained for each track. The best results for the first waypoint (wp1) to the second waypoint (wp2) were obtained at the accuracy of 88.3 %, steady state error -5.51 with a travel time of 12.2 seconds. For the movement from the second waypoint (wp2) to the third waypoint point (wp3), the best results were obtained with an accuracy rate of 100 %, steady state error -2.62 with a travel time of 15 seconds.

Other than that, the system generates a steady state error of 3.55% (-4.26 m), with the largest deviation of 10.55% (12.66 m) and an average accuracy of 83 % when tracing the movement from wp1 to wp2. In this case, the tendency of steady state error is 2.88% (3.45 m), the largest deviation is 7.28% (8.74 m) with an average accuracy of 93 % for tracing from wp2 to wp3.

The aircraft oscillation looks sufficiently large when entering the first waypoint point. This is caused by the starting point of activating the waypoint mode to point first, when the waypoint forms a bearing angle that is more than 90 ° from the angle of large bearings that causes a deviation in tracking the track. In addition, the aircraft's tendency to deviate from the coordinates at the waypoint is influenced by the x-axis translational state input obtained from GPS sensor readings. Here, they are included in the low-frequency category so that it is not balanced with changes in actual aircraft displacement on at that time [27]. However, the deviation that occurs is still limited in comparison to the given tolerance threshold. The tolerance limit of the system is 6 meters to the left and 6 meters to the right, with the plane's maneuvering slope when searching for waypoints is 15°. This is due to the tendency of the aircraft to decrease in altitude when maneuvering. To keep the plane from stalling maneuvering is given a maximum angle limit when turning and assisted with maintain height.

VII. CONCLUSION

In this work, the model design of control system using LQR methods in waypoint mission have been proven in experiment test. The results show that the system responses represent the performance of flying wing in the waypoint has good stability in maintaining and holding position from the path. Flying wing also produces a very low steady state error and high accuracy. These results indicate that LQR controller results in the robust characteristic of the plane.

REFERENCES

- [1] K. Nonami, *Autonomous Flying Robots*. Japan: Springer Japan, 2010, pp. 2-7.
- [2] T.K. Priyambodo, A.E. Putro, A. Dharmawan, "Optimizing control based on ant colony for quadrotor stabilization", *Jurnal of IEEE International Conference of ICARES*, 2015.
- [3] A. Majid, R. Sumiharto and S.B. Wibisono, "Identifikasi model dari pesawat udara tanpa awak sayap tetap jenis bixler", *IJEIS*, Volume 5, ISSN: 2088-3714, 2015, pp.43-54.
- [4] P.S. Ardiantara, R. Sumiharto and S.B. Wibowo, "Purwarupa control kestabilan posisi dan sikap pada pesawat tanpa awak menggunakan IMU dan algoritma fusion sensor kalman filter", *IJEIS*, 4(1), 2014, pp.25-34.
- [5] J. Osborne and R. Rysdyk, "Waypoint guidance for small UAVs in wind", AIAA Virginia, No. 6951, 2005.
- [6] R. Shaffer, M. Karpenko and Q. Gong, "Unscented guidance for waypoint navigation of a fixed-wing UAV," *2016 American Control Conference (ACC)*, Boston, MA, 2016, pp. 473-478, doi: 10.1109/ACC.2016.7524959.
- [7] S. Markin, "Multiple simultaneous specification attitude control of a mini flying-wing unmanned aerial vehicle", Graduate Department of Mechanical and Industrial Engineering, University of Toronto, 2010.
- [8] G. A. Venkatesh, P. Sumanth and K. R. Jansi, "Fully Autonomous UAV," *2017 International Conference on Technical Advancements in Computers and Communications (ICTACC)*, Melmaurvathur, 2017, pp. 41-44, doi: 10.1109/ICTACC.2017.20.
- [9] L.V. Santana, A.S. Brandao and M. Sarcinelli-Filho, "Outdoor waypoint navigation with the AR.Drone quadrotor", *International Conference on Unmanned Aircraft Systems (ICUAS) IEEE*, Juni, 2015, pp.303-311..
- [10] S. Kukreti, M. Kumar and K. Cohen, "Detection and localization using unmanned aerial systems for firefighting applications", *Conference AIAA Aerospace, At San Diego, CA*, Vol. AIAA SCITECH, 2016.
- [11] M. Fajar and O. Arifianto, "Perancangan autopilot lateral-direksional pesawat nirawak LSU-05", *Jurnal Teknologi Dirgantara*, Vol.15, 2005.
- [12] D. Stojcsics, "Autonomous Waypoint-based Guidance Methods for Small Size Unmanned Aerial Vehicles" *Acta Polytechnica Hungarica*, Vol.11, No. 10, 2014, pp. 215-233.
- [13] T. K. Priyambodo, A. Dharmawan, O. A. Dhewa dan N. A. S. Putro, "Optimizing control based on fine tune PID using ant colony logic for moving control of UAV systems", *American Institute of Physics Conference Proceedings* 1755, 170011, 2016.
- [14] N.A. Ismail, N.L. Othman, Z.M. Zain, D. Pebrianti and L. Bayuaji, "Attitude control of quadrotor", *ARNP Journal of Engineering and Applied Sciences*, Vol.10, No.22, 2015, pp.1726-1731.
- [15] O. A. Dhewa, A. Dharmawan and T. K. Priyambodo, "Model of linear quadratic regulator (LQR) control method in hovering state of quadrotor", *Journal of Telecommunication, Electronic and Computer Engineering*, Vol. 9, No. 3, 2017, pp. 135-143.
- [16] L.M. Argentim, W.C. Rezende, P.E. Santos and R.A. Aguiar, "PID, LQR and LQR-PID on a quadrotor platform", *International Conference on Informatics, Electronics and Vision (ICIEV) IEEE*, 2013.
- [17] E.C. Suicmez and A.T. Kutay, "Optimal path tracking control of a quadrotor UAV," *International Conference on Unmanned Aircraft Systems (ICUAS) IEEE*, 2014, pp.27-30.
- [18] R. C. Hibbeler, *Dynamics*. Hoboken, New Jersey: Pearson Prentice Hall, 2016.
- [19] J.G. Li, X. Chen, Y. Li and R. Zhang, "Control system design of flying-wing UAV based on nonlinear methodology" *Defence Technology*, 2017, 13. 10.1016/j.dt.2017.06.003.
- [20] C. Z. Myint, H. M. Tun and Z. M. Naing, "Development of Linear Quadratic Regulator Design for small UAV System", *International Journal of Scientific & Technology Research*, Vol. 5, Issue 07, 2016.
- [21] Whidborne, J.F, *Modelling and Linear Control of a Quadcopter*, Cranfield University, 2007.
- [22] G. Nugroho and A. Dharmawan, "Undesirable rolling minimization on the EDF missiles flight based on LQR methods," *2017 International Conference on Advanced Mechatronics, Intelligent Manufacture, and Industrial Automation (ICAMIMIA)*, Surabaya, 2017, pp. 85-90, doi: 10.1109/ICAMIMIA.2017.8387563.
- [23] A. Dharmawan, A. Ashari, and A. E. Putra, "Quadrotor flight stability system with Routh stability and Lyapunov analysis," in *AIP Conference Proceedings*, 2016, vol. 1755, p. 170007.
- [24] A. Dharmawan, A. Ashari, and A. E. Putra, "Translation Movement Stability Control of Quad Tiltrotor Using LQR and LQG," *Int. J. Intell. Syst. Appl.*, vol. 10, no. 3, 2018, pp. 10-21.
- [25] A. Dharmawan, A. E. Putra, I. M. Tresnayana and W. A. Wicaksono, "The Obstacle Avoidance System In A Fixed-Wing UAV When Flying Low Using LQR Method," *2019 International Conference on Computer Engineering, Network, and Intelligent Multimedia (CENIM)*, Surabaya, Indonesia, 2019, pp. 1-7, doi: 10.1109/CENIM48368.2019.8973292.
- [26] S. Ayyildiz and H. Yazici, "Pitch Control by LQR for Fixed Wing Aircraft during Microburst Encounter", *5th International Conference on Advances in Mechanical Engineering Istanbul*, 2019.
- [27] J. Gross, Y. Gu, Yu and M. Rhudy, "Fixed-Wing UAV Attitude Estimation Using Single Antenna GPS Signal Strength Measurements". *Aerospace*, 2016.